Interaction of Substrate Uridyl 3',5'-Adenosine with Ribonuclease A: A Molecular Dynamics Study

K. Seshadri,* V. S. R. Rao,‡ and Saraswathi Vishveshwara*

*Molecular Biophysics Unit, Indian Institute of Science, Bangalore 560012, India, and ‡LMMB-National Cancer Institute, Rockville, Maryland 20892 USA

ABSTRACT   A wealth of information available from x-ray crystallographic structures of enzyme-ligand complexes makes it possible to study interactions at the molecular level. However, further investigation is needed when i) the binding of the natural substrate must be characterized, because ligands in the stable enzyme-ligand complexes are generally inhibitors or the analogs of substrate and transition state, and when ii) ligand binding is in part poorly characterized. We have investigated these aspects in the binding of substrate uridyl 3',5'-adenosine (UpA) to ribonuclease A (RNase A). Based on the systematically docked RNase A-UpA complex resulting from our previous study, we have undertaken a molecular dynamics simulation of the complex with solvent molecules. The molecular dynamics trajectories of this complex are analyzed to provide structural explanations for varied experimental observations on the ligand binding at the B2 subsite of ribonuclease A. The present study suggests that B2 subsite stabilization can be effected by different active site groups, depending on the substrate conformation. Thus when adenosine ribose pucker is O4'-endo, Gln69 and Glu111 form hydrogen-bonding contacts with adenine base, and when it is C2'-endo, Asn71 is the only amino acid residue in direct contact with this base. The latter observation is in support of previous mutagenesis and kinetics studies. Possible roles for the solvent molecules in the binding subsites are described. Furthermore, the substrate conformation is also examined along the simulation pathway to see if any conformer has the properties of a transition state. This study has also helped us to recognize that small but concerted changes in the conformation of the substrate can result in substrate geometry favorable for 2',3' cyclization. The identified geometry is suitable for intraligand proton transfer between 2'-hydroxyl and phosphate oxygen atom. The possibility of intraligand proton transfer as suggested previously and the mode of transfer before the formation of cyclic intermediate during transphosphorylation are discussed.

INTRODUCTION

Bovine pancreatic ribonuclease (RNase A; EC 3.1.27.5) is an extensively studied enzyme (Richards and Wyckoff, 1971; Blackburn and Moore, 1982; Wlodawer, 1985; Eftink and Biltonen, 1987). It cleaves single-stranded RNA or a dinucleotide unit 3',5'-NpN in a two-step concerted acid-base mechanism (transphosphorylation and hydrolysis; Fig. 1 a) and is known to be specific for a pyrimidine nucleoside on the 3' side of the phosphodiester linkage that is hydrolyzed. The enzyme shows a small preference to a purine nucleoside on the 5' side of the linkage. Based on x-ray crystallographic investigations and biochemical studies on RNase A-ligand complexes, various binding subsites (viz., B1, R1, p1, R2, and B2) have been identified in this enzyme (where B stands for base, R for ribose, and p for phosphate; 1 refers to the 3' side of the phosphate and 2 refers to the 5' side) (Richards and Wyckoff, 1973; Mitsui et al., 1978; Pares et al., 1991). The structural studies of RNase A-dinucleotide complexes have pointed out in general terms, for the B2 subsite, that amino acid residues Gln69 and Glu111 interact with the purine base, with the possible involvement of Asn71 (Richards and Wyckoff, 1973; Wodak et al., 1977;

Pavlovsky et al., 1978; Wlodawer, 1985; Llorens et al., 1989). We have recently docked the substrate uridyl 3',5'-adenosine (UpA) shown in Fig. 2 in the active site of RNase A using systematic search, contact criteria, and energy minimization and have identified a suitable enzyme-substrate model (Fig. 3) based on energetics and experimental protein-ligand interactions, with implicit treatment of solvent molecules (Seshadri et al., 1994). This model has helped in characterizing various features such as ideal substrate conformation and atomic-level description of B2 subsite interactions of adenine base, which were unclear earlier. However, the more recent kinetic experiments by Tarragona-Fiol et al. (1993) present a somewhat different scheme of interactions at this subsite. Their studies indicate that for RNase A-UpA complex, productive interactions of the purine base must arise solely with Asn71, whereas Gln69 and Glu111 need not be functionally involved. This calls for further investigation to enhance our understanding of the stability of protein-ligand interactions at different subsites.

The catalytic reaction takes place via the formation of a 2',3'-cyclic phosphate intermediate (Usher et al., 1970, 1972). There have been several experimental (see, for example, Linquist et al., 1973; Borah et al., 1985) and theoretical (Gorenstein et al., 1977, 1979, 1987; Holmes et al., 1978; Holmes, 1980; Deakyne and Allen, 1979) approaches to describing the stereochemistry of the cyclization step and the possible involvement of certain active-site amino acid residues (viz., Gln11, His12, Asn44, His119, and Phe120).
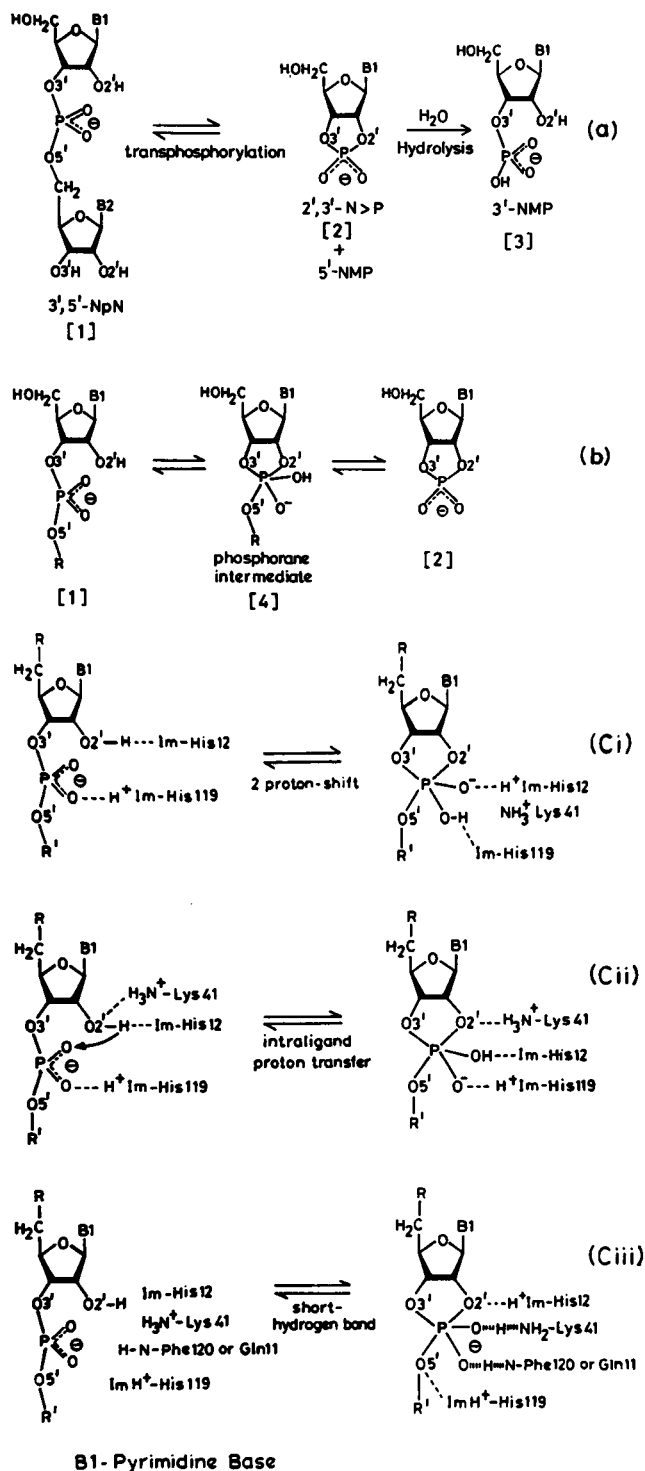

FIGURE 1 (a) Two major steps of NpN hydrolysis by RNase A. B1, pyrimidine base; B2, purine or pyrimidine base; N, nucleoside. (b) Transphosphorylation through phosphorane intermediate. (c) Mechanism of the formation of monoion-phosphorane intermediate. (i) Breslow's two-proton shift; (ii) Lim and Tole intraligand proton transfer; and (iii) Gerlt and Gassman short hydrogen bond
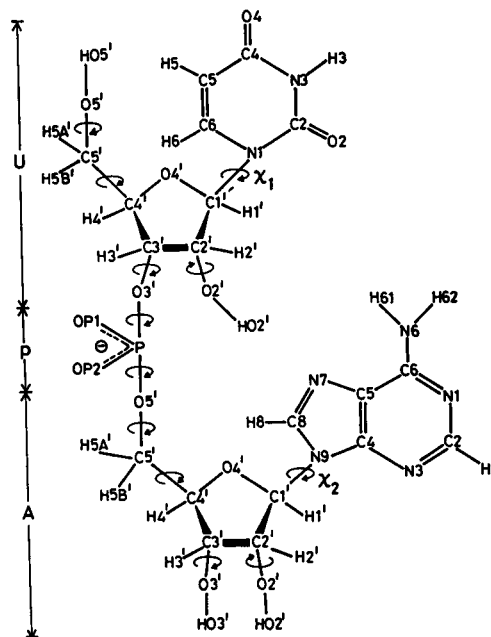

FIGURE 2 Schematic representation of UpA. Some of the rotations that are shown about the backbone and glycosidic bonds are discussed in the text and Table 1

1993) before the formation of the $2',3'$ cyclic intermediate as shown in Fig. 1 b (panel marked [4]). Based on the knowledge that His12 is located close to $2'$-hydroxyl and that His119 is near a phosphate oxygen in the active site, several mechanisms are proposed for the formation of the phosphorane intermediate. Three such recent proposals are summarized in Fig. 1 c. It is essential to know the precise location and position of different groups with respect to the substrate at the time of catalysis (Gerlt and Gassman, 1993). Apart from His12 and His119, although it is known that residues such as Lys41, Gln11, and Phe120 (NH-backbone) are in the vicinity of the cleavage site, how they reorient with respect to the substrate during intermediate formation is not clear from experimental studies. Hence several proposals are made for the mechanism of enzyme action. The proposal by Breslow and co-workers (Fig. 1 c-i) involves the simultaneous shift of two protons, one from His119 ND1(H) to phosphoryl oxygen and the other from O_2'(H) to His12 NE2. Lim and Tole (1992) have pointed out the inconsistency that will arise in pK_a values in Breslow's scheme. Based on the substrate-protein interactions obtained by molecular dynamics (MD) studies on RNase A-$2'$-deoxycytidyl-$3',5'$-adenosine (RNase A-CpA) complex by Haydock et al. (1990), they propose an intraligand proton transfer (assisted by His12) as shown in Fig. 1 c-ii. In the third mechanism proposed by Gerlt and Gassman (Fig. 1 c-iii), the focus is more on the stability of the monoion phosphorane intermediate through one or two short hydrogen bonds that delocalize the net charge on the substrate. Thus, it is clear that the knowledge of the mutual orientation of all the important substrate groups and the

By kinetic experiments Breslow and co-workers have arrived at monoionic phosphorane intermediate (Breslow and Labelle, 1986; Anslyn and Breslow, 1989; Breslow and Xu,
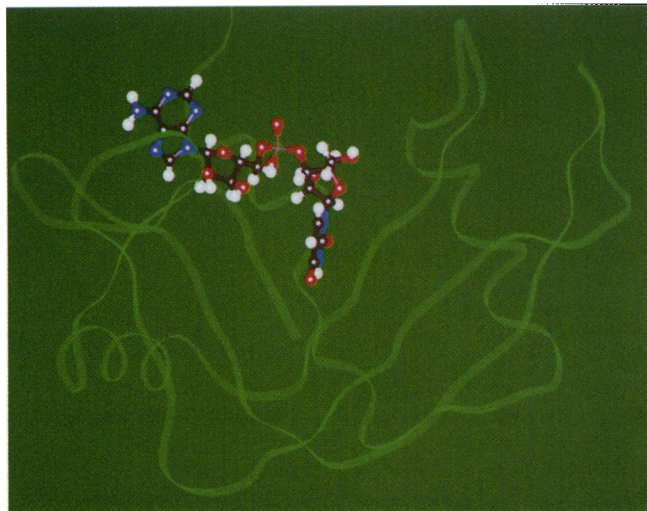
FIGURE 3　Ribbon drawing of productive RNaseA-UpA complex obtained in our earlier study (starting structure for the present MD study)

active-site protein residues is necessary to understand the precise mechanism of enzyme catalysis.

Analysis of dynamical properties of the explicitly solvated active site of this complex is expected to yield a more realistic description of the active-site phenomena. In the present report, we have carried out MD studies on RNase A-UpA complex, starting from our modeled structure and minimizing it with a sphere of solvent molecules centered at the phosphorus atom. The analysis of the structural trajectories has enabled us to identify transformation from a complex with all the recognized interactions, to conformations suitable for a) B2-subsite interactions in agreement with the findings of Tarragona-Fiol et al. (1993) and (b) the possible formation of the phosphorane intermediate through an intra-ligand proton transfer from 2'-hydroxyl to phosphoryl oxygen as proposed in the mechanism (Fig. 1 c-iii). The details of the investigations are given below.

MATERIALS AND METHODS

The present report forms a part of the series of investigations on RNase A-ligand complexes. The starting coordinates of RNase A were taken from the x-ray crystallographic study of native, phosphate free enzyme (Wlodawer et al., 1988). Based on RNase A-3'UMP conformers obtained by energy minimization studies (Seshadri et al., 1993), the substrate UpA was fitted in the active site by systematically varying the ribose pucker, both backbone and glycosidic torsion angles of the nucleoside on the 5' side of the phosphodiester linkage, along with the side chain torsion angles of the amino acid residues belonging to the B2 site. Subsequent energy minimization (Seshadri et al., 1994) allowed us to identify a conformer of the RNase A-UpA complex with productive enzyme-substrate interactions. A solvated, active site dynamics of the complex was modeled with AM-BER (assisted model building with energy refinement) suite of programs using "all atom" force field (Pearlman et al., 1991). All amino acid residues (whole or part) lying within 12 Å of the phosphorus atom of the cleavage site were included as belonging to the active site. Thus identified residues included the residues that are known to assist the substrate binding and enzyme activity (viz., His12, Lys41, Thr45, His119, Phe120, and Ser123). A spherical solvent cap of 15 Å was built around the phosphorus atom, in

which pre-equilibrated "Monte Carlo water molecules" numbering 173 were placed after steric and distance criteria. A harmonic force constant of 1.5 kcal/Å was used to restrain water molecules at the cap boundary. A dielectric constant of $\epsilon = 1$ was used to model the electrostatic interactions in the active site. Conjugate gradient minimization was then performed to relax the system to the AMBER force field (Weiner et al., 1984, 1986). In both minimization and subsequent MD, only the active-site residues, the substrate UpA, and all water molecules were allowed to move. A TIP3P water model was used for the solvent molecules in the simulation. The system was equilibrated in a stepwise fashion; the minimized structure was heated to a temperature of 50 K and equilibrated for 5 ps. This procedure was repeated for every additional 50 K until the system attained 300 K at 25 ps. The system was maintained at this temperature for additional 10 ps, and at 35 ps a production run was initiated and was conducted up to 145 ps. The energy profiles obtained under these conditions are given in Fig. 4. The simulation was a constant temperature dynamics, coupled to a heat bath at 300 K. The nonbonded interactions were updated every 10 steps, with a cut-off of 12 Å. The MD calculation was performed on an IBM-RISC 6000 computer. The trajectories of various torsion angles, hydrogen bonds, and ribose pucker, and statistical parameters were computed using in-house routines and adaptations.

RESULTS AND DISCUSSION

Substrate conformation

The substrate conformation is presented in terms of the pseudorotation phase angle of the riboses, the glycosidic torsion angles describing the orientation of the uracil and the adenine bases, and the backbone torsion angles about the bonds that connect the uridine and the adenine nucleosides. Some of the trajectories corresponding to these parameters are given in Fig. 5, a–d. The initial minimized geometry considered for the MD simulation, MD averages, and the RMS deviations are given in columns 2 and 3 of Table 1. All of the parameters reported in Table 1 fluctuate with RMS deviation less than 16°, with the exception of the free hydroxyl groups, which show considerable fluctuation from the average values. For the parameters that fluctuated around more than one conformation, separate average and RMS deviation values have been given. Certain selected distances are also displayed along with the minimum and maximum values attained during the simulation, in square enclosures.

The uridine ribose (ribose 1) essentially stays at C3'-endo throughout the simulation, whereas the adenosine ribose (ribose 2) shows a transition from O4'-endo to C1'-exo-C2'-endo twist pucker (henceforth, C2'endo region) at around 70 ps (Fig. 5 a). During the interval 120–130 ps such a transition is reversed and the ribose pucker tends to reach O4'-endo in the remaining part of the simulation. The glycosidic torsion angles of the pyrimidine and purine bases stay at anti and syn (+ sc) conformations, respectively (Fig. 5, b and c). However, the adenine base is more flexible. Its orientation (χ_2, Fig. 5 c) fluctuates considerably until about 80 ps, and it has also accessed the anti region during a 40–50-ps interval in the initial stage of the simulation. After 70 ps, it stabilizes around −90° (270°), which is correlated with the C2'-endo pucker of ribose 2. The phosphodiester bonds (UO3'-P-AO5') are stable at a distorted $(+g, -g)$

FIGURE 4 Energy profile of RNase A-UpA simulation under the conditions described in the text.
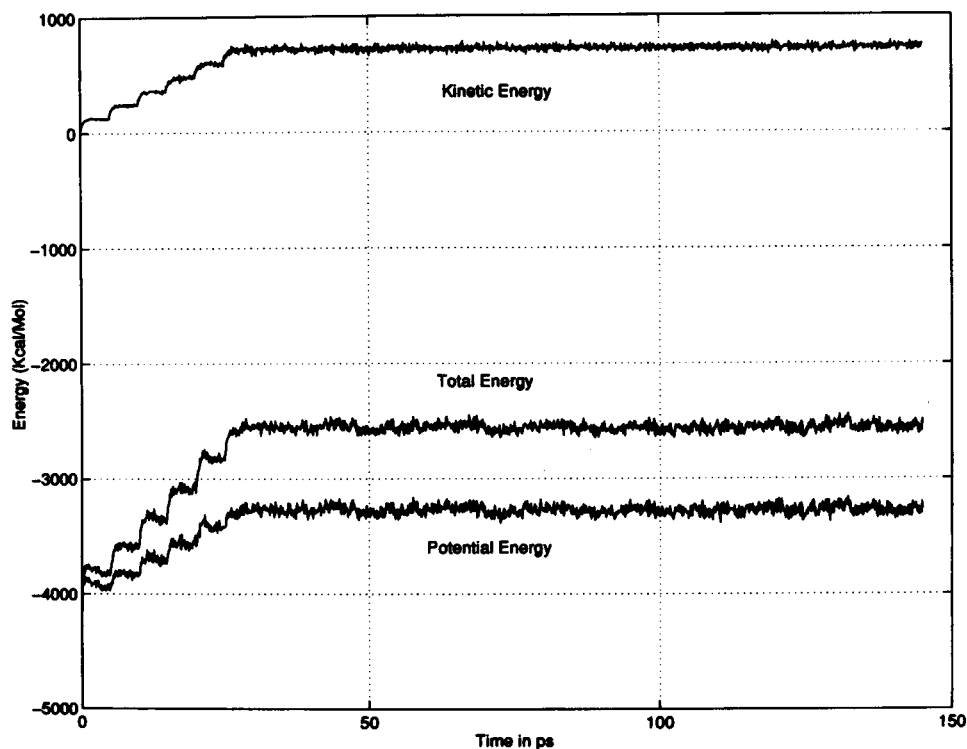
conformation. Such a mode of binding does not correspond to the best ligand energy but is essential for the best ligand-protein energetics, as revealed in our earlier study (Seshadri et al., 1994). The rotation around the bonds on either sides of this linkage, UC3'-UO3' and AO5'-AC5', are also stable at around $-172°$ and $-175°$, respectively. The rotation around AC5'-AC4' stays close to 170°, although at around 70 ps (Fig. 5 d) there seems to be a shift of about 20°, indicative of a conformational transition. Hence the simulation shows that the nucleotide segment from the uridine base to ribose 2 does not deviate very much from the starting geometry. However, ribose 2 undergoes a confor-

mational transition and correspondingly the second base (adenine) orientation and the linkage joining the phosphate-ribose 2 change their conformation during a 70–130-ps period.

Enzyme-substrate interaction

Selection of specific conformers

Apart from the frequent (every 0.1 ps) storage of the coordinates during the time course of the simulation, coordinates of selected conformers were also stored for special attention; this was done for the purpose of analyzing the different conformations accessed by RNase A-UpA complex, and this required an empirical exercise of identifying a minimum number of conformers to adequately represent the conformational properties of the system. For example, a conformer on either side of the transition point around 70 ps in the ribose pucker trajectory (Fig. 5 a, top) would fairly describe the conformation of adenosine ribose accessing O4'endo and C1'exo-C2'endo regions of pucker. Seven conformers thus chosen with a reasonable variation in the substrate dihedrals, ribose pucker, and hydrogen bonds involving substrate, protein, and the solvent correspond to 35.8, 45.2, 54.9, 73.2, 84.0, 115.6, and 127.5 ps. These conformers were subjected to minimization for 1000 cycles to enable them reach the local minima. The resultant substrate conformations are given in Table 1, and Table 2 presents the details of hydrogen bonding at different moieties of the ligand for these conformers. Fig. 6, a–i, represents some of the stable hydrogen bonds through MD distance trajectories.
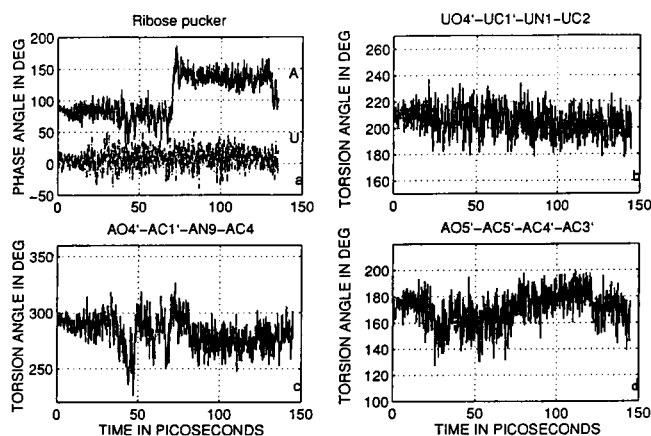

FIGURE 5   MD trajectories representing the substrate conformation. (a) Phase angle of adenosine (A) and uridine (U) riboses. (b) Torsion angle UO4'-UC1'-UN1-UC2. (c) Torsion angle AO4'-AC1'-AN9-AC4. (d) Torsion angle AO5'-AC5'-AC4'-AC3'

TABLE 1   Substrate conformation and selected distances in various energy minimized conformers chosen from MD study

	Initial minimized model	MD average	Minimized points along MD trajectory						
			35.8ps	45.2ps	54.9ps	73.2ps	84.0ps	115.6ps	127.5ps
Torsion angles (°):									
UO4'-UC1'-UN1-UC2 (χ1)	−1.57	−155 ± 9	−147	−162	−143	−153	−162	−159	−165
UHO5'-UO5'-UC5'-UC4'	−175	−128 ± 80	162	−151	179	−110	−51	−38	48
UO5'-UC5'-UC4'-UC3'	−174	173 ± 14	−174	178	−173	167	157	170	173
UC5'-UC4'-UC3'-UO3'	88	87 ± 7	86	91	86	88	87	88	89
UC1'-UC2'-UO2'-UHO2'	126	128 ± 22	108	115	156	115	118	101	113
UC4'-UC3'-UO3'-P	−161	−172 ± 10	−175	−171	177	−161	−168	180	−155
UC3'-UO3'-P AO5'	80	90 ± 8	85	90	79	91	92	101	86
UO3'-P AO5'-AC5'	−77	−71 ± 10	−85	−70	−70	−75	−67	−71	−71
P-AO5'-AC5'-AC4'	−165	−175 ± 9	−163	−171	−172	176	−174	−177	−178
AO5'-AC5'-AC4'-AC3'	164	171 ± 12	175	160	171	169	173	−172	165
AC5'-AC4'-AC3'-AO3'	92	87 ± 8 132 ± 11	92	91	86	154	118	132	134
AC4'-AC3'-AO3'-AHO3'	178	157 ± 29 −33 ± 76	177	179	158	140	111	145	136
AC3'-AC2'-AO2'-AHO2'	−172	−68 ± 17 12 ± 24 −171 ± 8	−55	−56	−61	−83	−79	−86	−78
AO4'-AC1'-AN9-AC4 (χ2)	−62	−78 ± 13	−61	−90	−61	−61	−82	−85	−80
Ribose phase angle (°):									
i) Uridine Ribose	6	8 ± 14	13	7	9	11	13	6	9
ii) Adenosine Ribose	91	83 ± 16 139 ± 11	91	93	80	163	125	135	137
Some distances:									
O2' ... P (d1)	3.58	3.47 ± 0.16 [2.95, 4.04]	3.41	3.39	3.27	3.61	3.52	3.35	3.65
UO2' ... UOP1 (d2)	3.50	3.39 ± 0.22 [2.67, 4.10]	3.29	3.30	2.88	3.66	3.49	3.40	3.74
UHO2' ... UOP1 (d3)	3.25	3.11 ± 0.37 [1.89, 4.54]	3.22	3.16	2.13	3.60	3.33	3.44	3.71
UOP1 ... F120 HN	1.69	1.82 ± 0.14 [1.57, 2.85]	1.82	1.74	2.62	1.67	1.70	1.74	1.71
UHO2' ... H12 NE2	1.90	2.26 ± 0.34 [1.72, 4.51]	1.91	1.90	2.96	1.91	1.96	2.15	1.91

Four hydrogen bonds that stabilize the B1 subsite are made by the backbone and side chains of Thr45 and Ser123 with the uracil base at positions 2, 3, and 4. They are UO$_2$ ... Thr45 HN, UH3 ... Thr45 OG1, UO4 ... Ser123 HN, and UO4 ... Ser123 HOG. The interaction of the backbone amide NH of Thr45 with O$_2$ of uracil, depicted in Fig. 6 a, is more stable than the rest. The 2'-hydroxyl group is the major promoter of hydrogen bonding stability of the ribose at the 3' side of the phosphodiester linkage, interacting with the side chains of the residues such as His12 and Lys41, as seen in Fig. 6, b and c. The interaction of phosphate (OP1) with the backbone of Phe120(NH) is extremely stable (Fig. 6 d). This has been recognized as RNase A-ligand anchoring interaction from the previous minimization studies (Seshadri et al., 1994). Other hydrogen bonds that are formed with the phosphate oxygens are by the side chains of Gln11 and His119. Whereas the Gln11 HE2 ... OP2 (Fig. 6 e) hydrogen bond is stable throughout the simulation, His119 interacts with the phosphate group through OP2 (Fig. 6 f) and AO5' (Fig. 6 h) atoms. It also interacts with a water molecule (W215) (Fig. 6 g). HD1 of His119 either hydrogen bonds with OP2 and AO5' or with

water. The interactions of His119 with OP2 and AO5' are highly correlated, whereas the interactions of this residue with AO5' and the water molecule (W215) are highly anticorrelated, as shown in Table 3. The water molecule, however, moves closer to the phosphate group after 80 ps, as seen in Table 2. In the B2 binding subsite Gln69, Asn71 and Glu111 interact with the adenine base. In the first 70 ps of the simulation time, Gln69 and Glu111 can have direct but unstable interaction with the adenine base (trajectories are not shown; however, they can be seen from interactions presented in Table 2). Between 70 and 120 ps Asn71 has very stable interaction at positions six and seven of the purine base, as clearly shown in Table 2 and, representatively, in Fig. 6 i. In fact, such a behavior is highly anticorrelated with the conformational transitions that occur in the 5' side of the substrate during this time, more notably in the adenosine ribose pucker (Table 3). This is in agreement with the recent site-directed mutation experimental results (Tarragona-Fiol et al., 1993) in which Asn71 is the only residue of B2 subsite found to affect K_{cat} of the reaction catalyzed by RNase A. It is discussed in detail in the following section.

TABLE 2 Details of hydrogen bonding in energy minimized conformers of Table 1

Substrate-enzyme hydrogen bonds:	Initial minimized model	Minimized points along MD trajectory						
		35.8 ps	45.2 ps	54.9 ps	73.2 ps	84.0 ps	115.6 ps	127.5 ps
Uracil base								
UO2	T45 HN	T45 HN	T45 HN	T45 HN	T45 HN	T45 HN	T45 HN	T45 HN
UH3	T45 OG1	T45 OG1			T45 OG1		T45 OG1	
UO4	S123 HN	S123 HN	S123 HN	S123 HN	S123 HN	S123 HOG	S123 HN	S123 HOG
		S123 HOG	S123 HOG		S123 HOG		S123 HOG	
Uridine ribose								
UHO5'		W220 O	W230 O	W148 O	W232 O			W216 O
UO5'		W148 H1	W148 H2	W149 H2	W152 H2	W170 H2		
						W176 H2		
UO2'	K41 HNZ3	K41 HNZ3	K41 HNZ3	K41 HNZ1	K41 HNZ1	K41 HNZ1	K41 HNZ1	K41 HNZ1
UHO2'	H12 NE2	H12 NE2	H12 NE2		H12 NE2	H12 NE2	H12 NE2	H12 NE2
UO3'			W265 H1		W244 H2	W222 H2	W280 H1	
					W263 H2	(O -Q11 HNE2)	(O -K41 HNZ2)	
						(O -K41 HNZ1)		
Phosphate								
OP1	F120 HN	F120 HN	F120 HN	W215 H2	F120 HN	F120 HN	F120 HN	F120 HN
				(O -H119 HD1)				
OP2	K7 HNZ2	K7 HNZ3	K7 HNZ2	K7 HNZ2	K7 HNZ3	Q11 HNE1	Q11 HNE1	Q11 HNE1
	Q11 HNE1	Q11-HNE1	K7 HNZ3	W169 H1	Q11 HNE1	H119 HD1	W155 H1	H119 HD1
	H119 HD1	W222 H1	Q11 HNE1	W175 H1	H119 HD1	W215 H2	W215 H2	W155 H1
			W265 H1	(O -H119 HD1)		W223 H2	(H1-Q11 OE1)	W215 H2
						(O -H119 HD1)	(O -H119 HD1)	(H2-Q11 OE1)
							W280 H1	(O -H119 HD1)
							(O -K41 HNZ2)	
Adenosine ribose								
AO5'		W222 H1	W244 H2	W244 H1	W264 H2	H119 HD1	W223 H1	W184 H1
		W297 H1						
AO4'			W244 H2	W244 H1	W264 H2			W184 H1
AO3'	W258 H1	W210 H2	W168 H2	W211 H1		W220 H2	W200 H2	
				(H2-D121 O)			W289 H2	
AHO3'	D121 OD1	D121 OD1	D121 OD1	D121 OD1		W184 O		
AO2'	N67 HN	N67 HN	N67 HN	K66 HN	N67 HN	N67 HN	N67 HN	N67 HN
	W258 H1			N67 HN				
AHO2'	N67 OD1	D121 OD1	D121 OD1	D121 OD1		D121 OD1	D121 OD1	D121 OD1
Adenine base								
AN1	W233 H1	W236 H1	W168 H2		W250 H2	W252 H2	W168 H2	W2 OB H1
	W236 H1				(O -H119 HD1)		W167 H2	W245 H2
							(H1-E111 OE1)	
							(O -H119 HD1)	
AN3	W213 H1	W237 H1	W155 H2	W244 H2	W183 H2	W183 H2	W212 H2	W183 H2
								W184 H2
AH61	W250 O	W252 O	W188 O	W168 O		W282 O	W282 O	W168 O
	(H2-E111 OE1)			(H2-E111 OE1)		(O -Q69 HNE1)		
AH62	E111 OE2	E111 OE2	E111 OE2	E111 OE2	W185 O	N71 OD1	N71 OD1	W282 O
					(H1-E111 OE2)			(O -Q69 HNE1)
					(O -N71 HND2)			(H2-N71 OD1)
					(H2-N71 OD1)			
AN7	Q69 HNE2	W282 H2	W282 H1	W282 H2	W282 H2	N71 HND2	N71 HND2	W250 H2
		(O -N67 HND2)	(O -N67 HND2)	(O -N67 HND2)	(O -N67 HND2)			(O -N71 HND2)
		(O -Q69 HNE1)	(H2-N71 OD1)	(O -Q69 HNE1)	(O -Q69 HNE1)			(H1-E111 OE1)
				(H1-N71 OD1)				

'W' indicates water molecule; W258 means water molecule with residue serial number 258 and so on. 'O' and 'H' that follow represent oxygen and hydrogen atoms of the water molecule.

The hydrogen bonds of water molecules that interact with both the substrate and the enzyme are indicated in brackets.

Role of water

The hydrogen bonding details given in Table 2 indicate that the primary binding subsites B1 and R1 that accommodate the pyrimidine base and ribose are almost insulated from the solvent molecules. The interactions at p1, R2, and B2 subsites, however, are influenced considerably by the presence of water molecules. Such characteristic occupation by water molecules provides a measure of the space accessible in the R2 and B2 subsites. The availability of room in these subsites perhaps induces conformational changes observed in the adenosine as against its uridine counterpart.

An analysis of the hydrogen bonds between the active site residues, the substrate, and the solvent molecules in the minimized structures were carried out. The rearrangement
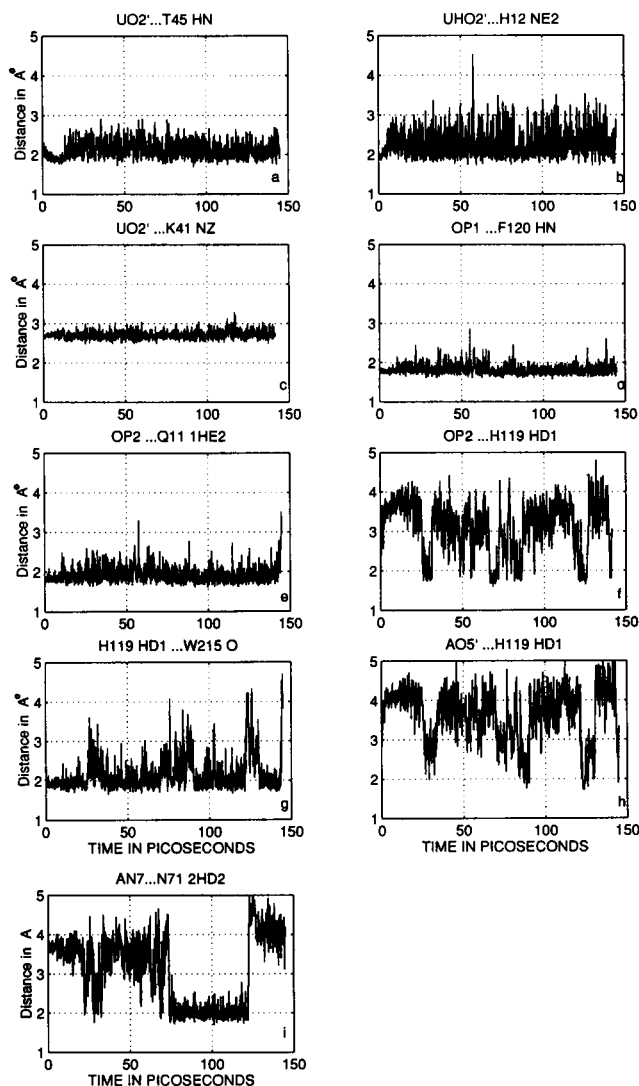
UO2'...T45 HN

UHO2'...H12 NE2

UO2'...K41 NZ

OP1 ...F120 HN

OP2 ...Q11 1HE2

OP2 ...H119 HD1

H119 HD1 ...W215 O

AO5' ...H119 HD1

TIME IN PICOSECONDS

TIME IN PICOSECONDS

AN7...N71 2HD2

TIME IN PICOSECONDS

FIGURE 6 MD trajectories of some contact distances involving substrate, enzyme, and the solvent molecules. (a) UO_2 ... Thr HN; (b) UHO_2' ... His12 NE2; (c) UO_2' ... Lys41 NZ; (d) OP1 ... Phe120 HN; (e) OP2 ... Gln11 1H2; (f) OP2 ... His119 HD1; (g) His119 HD1 ... Water 215 O; (h) AO5' ... His119 HD1; (i) AN7 ... N71 2HD2.

TABLE 3 Correlation coefficient (σ) between various interaction parameters* among RnaseA-U_pA-water

Interactions	σ
OP2 ... His 119—His 119 ... Water 215 (Fig. 6, f–g)	−0.484
OP2 ... His 119—His 119 ... .AO5' (Fig. 6, f–h)	0.814
His 119 ... Water 215—His 119 ... AO5' (Fig. 6, g–h)	−0.725
AN 7 ... N 71-Pucker angle (Figs. 6i–5a (A))	−0.475

*Distances between interacting groups with the exception of pucker angle for the adenosine ribose of U_pA.

when a nucleotide of sort UpA binds to RNase A. The structural details available from the present MD simulation assume significance in the light of their experiments. It is realized that in the conformers corresponding to 84.0 ps and 115.6 ps the only amino acid that stabilizes the adenine base through hydrogen bonding is Asn71. As revealed from Fig. 6 i, Asn71 is placed in position to have stable interaction with adenine for a considerable period of simulation time when the adenosine ribose flips to the C2'endo region. The hydrogen bond contacts made by Gln69 and Glu111 are weakened during this time. However, as seen in Table 2, the dynamic character of the solvent at this subsite is helpful in establishing a "mediated bridge" between these side chains and the purine base. Such a finding provides a rational basis for an explanation of varied experimental observations in this undercharacterized binding site. Also, because many interactions in the B2 subsite are water mediated, it explains why interactions at this subsite are not as well characterized as B1 subsite interactions.

There are certain differences in the results between the earlier minimization (Seshadri et al., 1994) and the present solvated active site dynamics, primarily because of the effect of solvation. The catalytically important uridine 2'-hydroxyl group has strengthened its interaction with His12 in the presence of water, at the expense of its hydrogen bond with Asn44. A water molecule is seen to compete with His119 in its interaction with phosphate groups, which may be vital from the catalytic point of view. The direct interaction of B2 subsite residues such as Gln69 and Glu111 with adenine bases is mediated through water molecules.

Mechanistic implications

The first step of RNA cleavage is transphosphorylation where the 2',3' cyclic phosphate is formed through a phosphorane intermediate. The results of the present MD simulation are analyzed from this point of view. Although the proposed mechanisms for the formation of phosphorane intermediate (Fig. 1 c) differ in details, all of them require the UO_2' ... P distance (d1) to be the smallest for cyclization. Furthermore, it is known that the geometric constraint of the ribose ring increases the entropic advantage of cyclization by holding the 2'-hydroxyl in close proximity to P

of water molecules and side chain orientations, as a consequence of different adenosine ribose and base conformations, was observed in R2 and B2 subsites. When the ribose is near the C2'endo region, this part of the substrate is surrounded by a solvent chain that runs between the phosphate and base moieties. One of the water molecules mediates the interaction between His119 and the phosphate group.

The recent findings of Tarragona-Fiol et al. (1993) based on mutagenesis and kinetic experiments apparently lead us to rethink about the results obtained on B2 subsite binding interactions, from several structural studies (Richards and Wyckoff, 1973; Wodak et al., 1977; Pavlovsky et al., 1978; Wlodawer, 1985; Llorens et al., 1989). According to this report, Gln69 and Glu111, hitherto considered important for adenine binding, are not essential for productive interactions. They further infer that Asn71 is solely important

(Thatcher and Kluger, 1989). During the dynamics, we monitored $d1$ along with the distance between UO_2^- and OP1 ($d2$) (OP1 is always closer to UO_2^- than OP2). The distances range generally between 2.95 and 4.04 Å for $d1$ and between 2.67 and 4.10 Å for $d2$. The lowest value for $d2$ occurs at 54.9 ps, when $d1$ takes up 3.16 Å, a value considerably lower than the average (3.47 Å) as given in Table 1, and such a distance establishes a hydrogen bond UO_2^--UHO_2^- ... OP1 (UHO_2^- ... OP1 distance ($d3$) is 1.89 Å). The UpA conformation at this point is favorable for the transfer of protons from 2'-hydroxyl to the phosphoryl oxygen OP1 as suggested by intra-substrate proton transfer by Lim and Tole (see Fig. 1 c-ii).

Among the hydroxyl groups of the substrate, 2'-hydroxyl is somewhat restricted, and this has a bearing on the UHO_2^- ... OP1 distance trajectory. The values for $d1$, $d2$, and $d3$ in the conformer picked at 54.9 ps and minimized are 3.27, 2.88, and 2.13 Å, respectively. A comparison of conformational parameters of UpA corresponding to the energy minimized starting model for MD and the structure at 54.9 ps shows that the backbone and the glycosidic torsion angles and the uridine ribose pucker, which are responsible for the maintenance of 2'-hydroxyl and phosphate groups at the observed positions, are roughly in the same region. Even though this is the case, there is sufficient flexibility in the substrate and $d1$ can vary from 2.95 to 4.04 Å. Hence small but concerted changes in these parameters can be significant in the actual positioning of the groups that take part in the catalysis.

The enzyme-substrate interaction for the minimized structure corresponding to 54.9 ps is analyzed and compared with respect to the rest of the trajectory. A ribbon representation of the active site of this structure is given in Fig. 7 a, which clearly shows 2'-hydroxyl hydrogen orienting toward the phosphoryl oxygen, which, during most of the simulation period, points in the direction of NE2 of His12 (Fig. 7 b). The hydrogen bonding contacts made by the amino acid residues Lys41(HNZ ... UO_2^-), Thr45(HN ... UO_2), Glu111(OE ... AH6), and Ser123 (HN ... UO4) over almost the entire simulation time are also seen in the conformer at 54.9 ps. However, interactions such as Gln11 HNE ... OP2, His12 NE2 ... UHO_2^-, Thr45 OG1 ... UH3, and Phe120 HN ... OP1, which promoted the stability of the RNase A-UpA complex during the majority of the MD simulation period, are somewhat weakened in this conformer. This conformer is marked by a characteristic rearrangement of the hydrogen bonding interaction network in the phosphodiester-2'-hydroxyl region, which achieves a putative transition-state-like conformation. The present study offers a model for intra-ligand proton transfer mechanism; however, it should be noted that the conventional mechanism of proton transfer through His12 is not ruled out, because the UHO_2' group is generally around hydrogen bonding distance from His12 (Fig. 6 b).

The differences between the present simulation and the study of Haydock et al. (1990) of the RNase A-CpA complex are perhaps noteworthy. The x-ray crystal structure of the RNase A-dCpA complex (Petsko and co-workers, 1984,
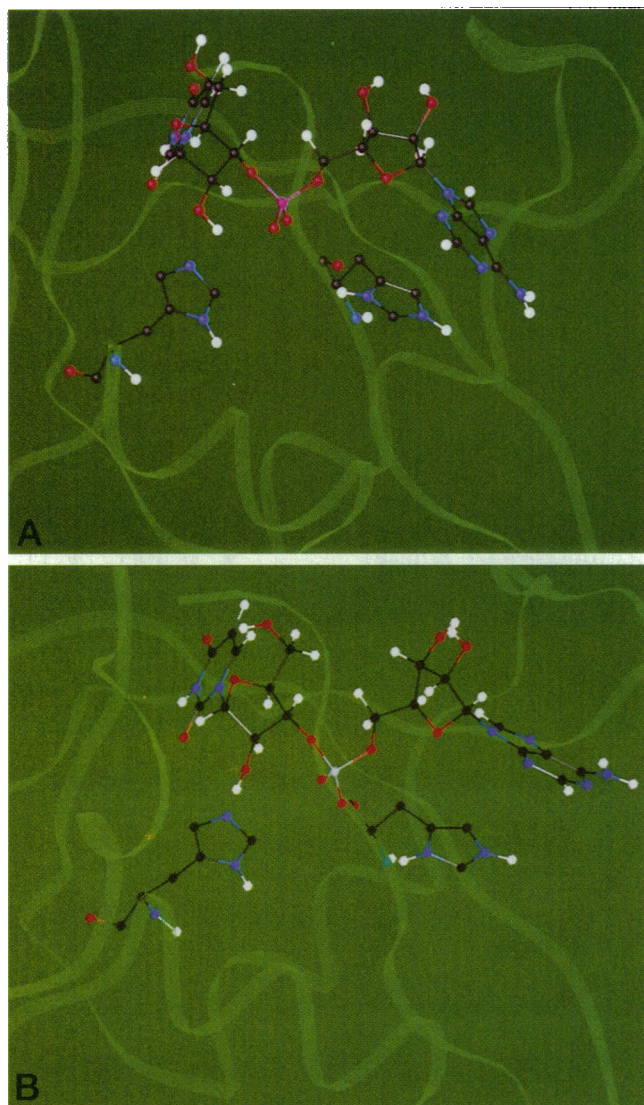
FIGURE 7   (a) Ribbon drawing with details of cleavage site of RNase A-UpA complex corresponding to 54.9 ps structure. Phosphorus atom is shown in pink. 2'-OH group is oriented toward phosphoryl oxygen. His12 is shown on the left bottom; His119 is on the right bottom stacking with Phe120. (b) Similar drawing corresponding to 115.6 ps structure. In contrast to the above orientation, 2'OH group hydrogen bonds to His12.

details and coordinates unpublished) formed the initial model for the MD simulation by Haydock et al. (1990), whereas the present study rests upon systematic docking coupled with energy minimization for the initial structure. The protein-nucleotide interactions obtained from both of these studies match in general with each other regarding interactions at the B1 subsite (Thr45, Ser123 ... pyrimidine base), the R1 subsite (His12, Lys41 ... pyrimidine ribose), and the p1 subsite (His119, Phe120 ... phosphate moiety). However, the details and organization of hydrogen bonds involving Gln11, His119, and Phe120 with the crucial phosphate group differ. Fig. 8, a–c, distinguishes these features in a schematic way. Fig. 8 a presents a minimized initial model taken for our study that can be compared with Fig. 8

b, which is drawn following the details given by Haydock et al. (1990). The phosphodiester conformation (120°, −60°) in the structure shown in Fig. 8 *b* orients the phosphoryl oxygens in such a way as to bring one of them (OP1) within hydrogen bonding distance of both His119 HD1 and Phe120 HN. In our initial model (Fig. 8 *a*) the phosphodiester conformation is (80°, −77°), and it fluctuates around this value during MD simulation (Table 1). Furthermore, His119 and Phe 120 interact with different oxygens (OP2 and OP1, respectively) of the phosphate group. The interaction of Phe120 HN ... OP1 is stable except during 54.9 ps (Table 2). On the other hand, the interaction of His119 with OP2 is often mediated through water. The observed deviations in the two simulations are perhaps due to small differences in the starting structure; a significant difference is in the adaptation of the phosphate group in the absence of the 2'-hydroxyl group in the x-ray crystallographic structure. This indicates that subtle differences in the interaction at the atomic level crucial for binding and catalysis may not be properly identified by studies that replace a substrate by inhibitors. The starting point of the present simulation yielded a transition-state-like structure at 54.9 ps (Fig. 8 *c*), which is significant from the mechanism point of view. Furthermore, more details at the atomic level are available from our study. It has offered details regarding the flexibility involved in the substrate conformation and the interaction of the second base with the protein side chains; the present study indicates an unusual ribose pucker (O4'-endo) for the second ribose. Also, the involvement of water molecules as bridges between substrate and protein in the B2 subsite has emerged from the present study.

SUMMARY

The MD study of the RNase A-UpA complex has allowed us to examine the conformational flexibility of the substrate at the active site. The uridine nucleoside in the RNase A-UpA complex exhibits stability with C3'-endo, anti conformation, whereas its adenosine counterpart undergoes a conformational transition at around 70 ps. Thus the 5' side nucleoside displays two conformations: O4'-endo; syn(+ sc) and C2'-endo (syn(+ sc) with more flexibility). From the present studies, it has also been possible to identify the role and accessibility of the solvent molecules in the binding subsites with a special relevance to the hitherto undercharacterized B2 binding subsite. The subsites p1, R2, and B2 are more hydrated compared to B1 and R1. The x-ray crystallographic observations of the interaction patterns between Gln69 and Glu111 and the adenine base are possible when the adenosine ribose adopts a O4'-endo pucker; on the other hand, when the ribose switches over to the C2'-endo

FIGURE 8 Schematic drawings of enzyme-substrate interactions based on (*a*) initial model for MD corresponding to Fig. 3; (*b*) 20 ps dynamics average structure of Haydock et al. (1990); (*c*) minimized structure at 54.9 ps of MD corresponding to Fig. 7 *a*.

region, only Asn71 can have a direct contact with the purine base, in support of the kinetic data. Often some of the important enzyme-substrate contacts are mediated by solvent molecules. Furthermore, the MD study has enabled us to identify a putative intermediate structure that is favorable for intra-substrate proton transfer from 2'-hydroxyl to phosphate oxygen. This offers a possible model for the mechanism proposed by Lim and Tole (1992) for the formation of 2',3' cyclic phosphorane intermediate during the transphosphorylation step of RNA hydrolysis by RNase A assisted by His12 (Fig. 1 c-ii). However, in the present simulation, several groups such as NE2 of His12 and NZ of Lys41 are around hydrogen bonding distance from the 2'-hydroxyl group for most of the time, which does not rule out other possible mechanisms of proton transfer. The present studies of the RNaseA-UpA complex essentially show that with a good starting complex structure, the atomic details and the dynamics of enzyme-substrate interactions can be meaningfully elaborated by MD simulations.

REFERENCES

Anslyn, E., and R. Breslow. 1989. On the mechanism of catalysis by ribonuclease: cleavage and isomerization of the dinucleotide UpU catalyzed by imidazole buffers. *J. Am. Chem. Soc.* 111:4473–4482.

Blackburn, P., and S. Moore. 1982. Pancreatic ribonuclease. *In* The Enzymes, Vol. XV. P. D. Boyer, editor. Academic Press, New York. 317–433.

Borah, B., C. W. Chen, W. Egan, M. Miller, A. Woldawer, and J. S. Cohen. 1985. Nuclear magnetic resonance and neutron diffraction studies of the complex of ribonuclease A with uridine vanadate, a transition-state analogue. *Biochemistry.* 24:2058–2067.

Breslow, R., and M. Labelle. 1986. Sequential general base-acid catalysis in the hydrolysis of RNA by imidazole. *J. Am. Chem. Soc.* 108:2655–2659.

Breslow, R., and R. Xu. 1993. Recognition and catalysis in nucleic acid chemistry. *Proc. Natl. Acad. Sci. USA.* 90:1201–1207.

Deakyne, C. A., and L. C. Allen. 1979. Role of active-site residues in the catalytic mechanism of ribonuclease A. *J. Am. Chem. Soc.* 101:3951–3959.

Eftink, M. R., and R. L. Biltonen. 1987. Pancreatic ribonuclease A: the most studied endonuclease. *In* Hydrolytic Enzymes. A. Neuberger and K. Brocklehurst, editors. Elsevier, Amsterdam. 333–376.

Gerlt, J. A., and P. G. Gassman. 1993. Understanding the rate of certain enzyme catalyzed reactions: proton abstraction from carbon acids, acyl-transfer reactins and displacement reactions of phosphodiesters. *Biochemistry.* 32:11943–11952.

Gorenstein, D. G., A. Chang, and J.-C. Yang. 1987. A reaffirmation of stereoelectronic control in the alkaline hydrolysis of methyl and ethyl ethylene phosphate. *Tetrahedron.* 43:469–478.

Gorenstein, D. G., B. A. Luxon, and J. B. Findlay. 1979. Stereoelectronic effects in the reactions of phosphate diesters. *Ab initio* molecular orbital calculations of reaction surfaces, 2. *J. Am. Chem. Soc.* 101:5869–5875.

Gorenstein, D. G., B. A. Luxon, J. B. Findlay, and R. Momii. 1977. Stereoelectronic effects in the hydrolysis of cyclic five-membered-ring phosphate esters. *Ab initio* and CNDO molecular orbital calculations on alkyloxyphosphoranes. *J. Am. Chem. Soc.* 99:4170–4172.

Haydock, K., C. Lim, A. T. Brunger, and M. Karplus. 1990. Simulation analysis of structures on the reaction pathway of RNase A. *J. Am. Chem. Soc.* 112:3826–3831.

Holmes, R. R. 1980. Pentacoordinated phosphorus. *In* ACS Monographs, Vol. II. Washington, DC. 176–180.

Holmes, R. R., J. A. Deiters, and J. C. Gallucii. 1978. Computer simulation of ribonuclease action on uridylyl-(3'-5')-adenosine. *J. Am. Chem. Soc.* 100:7393–7402.

Lim, C., and P. Tole. 1992. Endocyclic and exocyclic cleavage of phosphorane monoanion: a detailed mechanism of the RNase A transphosphorylation step. *J. Am. Chem. Soc.* 114:7245–7252.

Linquist, R. N., J. L. Lynn, and G. E. Leinhard. 1973. Possible transition-state analogs for ribonuclease: the complexes of uridine with oxovanadium (IV) ion and vanadium (V) ion. *J. Am. Chem. Soc.* 95:8762–8768.

Llorens, R. D., C. Arus, X. Pares, and C. M. Cuchillo. 1989. Chemical and computer graphics studies on the topography of the ribonuclease A active site cleft. A model of the enzyme-pentanucleotide substrate complex. *Protein Eng.* 2:417–429.

Mitsui, Y., Y. Urata, K. Torii, and M. Irie. 1978. Studies on the binding of adenylyl-3',5'-cytidine to ribonuclease. *Biochim. Biophys. Acta.* 535: 299–308.

Pares, X., M. V. Nogues, R. D. Llorens, and C. M. Cuchillo. 1991. Structure and function of ribonuclease A binding subsites. *In* Essays in Biochemistry, Vol. II. K. F. Tipton, editor. Portland Press, London. pp 89–103.

Pavlovsky, A. G., S. N. Borisova, V. V. Borisov, I. V. Antonov, and M. Ya. Karpeisky. 1978. The structure of the complex of ribonuclease S with fluoride analogue of UpA at 2.5 Å resolution. *FEBS Lett.* 92:258–262.

Pearlman, D. A., D. A. Case, J. C. Caldwell, G. L. Seibel, U. C. Singh, P. Weiner, and P. Kollman. 1991. AMBER 4.0. University of California, San Francisco.

Richards, F. M., and H. W. Wyckoff. 1971. Bovine pancreatic ribonuclease. *In* The Enzymes, Vol. IV. P. D. Boyer, editor. Academic Press, New York. 647–806.

Richards, F. M., and H. W. Wyckoff. 1973. Ribonuclease S. *In* Atlas of Molecular Structures in Biology, Vol. I. D. C. Phillips and F. M. Richards, editors. Clarendon Press, Oxford.

Seshadri, K., P. V. Balaji, V. S. R. Rao, and S. Vishveshwara. 1993. Computer modelling studies of ribonuclease A-pyrimidine nucleotide complexes. *J. Biomol. Struct. Dyn.* 11:395–415.

Seshadri, K., V. S. R. Rao, and S. Vishveshwara. 1994. Characterization of substrate UpA binding to ribonuclease A: a computer modelling and energetics approach. *J. Biomol. Struct. Dyn.* 12:581–603.

Tarragona-Fiol, A., H. J. Eggette, S. Harbron, E. Sanchez, C. J. Taylorson, J. M. Ward, and B. R. Rabin. 1993. Identification by site-directed mutagenesis of amino acids in the B2 subsite of bovine pancreatic ribonuclease A. *Protein Eng.* 6:901–906.

Thatcher, G. R. J., and R. Kluger. 1989. Mechanism and catalysis of nucleophilic substitution in phosphate esters. *Adv. Phys. Org. Chem.* 25:212–230.

Usher, D. A., E. S. Erenrich, and F. Eckstein. 1972. Geometry of the first step in action of ribonuclease A. *Proc. Natl. Acad. Sci. USA.* 69:115–118.

Usher, D. A., D. I. Richardson, Jr., and F. Eickstein. 1970. Absolute stereochemistry of the second step of ribonuclease action. *Nature.* 228:663–665.

Weiner, P. K., U. C. Singh, P. A. Kollman, J. Caldwell, and D. A. Case. 1981. A Molecular Mechanics and Dynamics Program: AMBER. University of California, San Francisco.

Weiner, S. J., P. A. Kollman, D. A. Case, U. C. Singh, C. Ghio, G. Alagona, S. Profeta, Jr., and P. Weiner. 1984. A new forcefield for molecular mechanical simulations of nucleic acids and proteins. *J. Am. Chem. Soc.* 106:765–784.

Weiner, S. J., P. A. Kollman, D. T. Nguyen, and D. A. Case. 1986. An all atom force field for simulations of proteins and nucleic acids. *J. Comp. Chem.* 7:230–252.

Wlodawer, A. 1985. Structure of bovine pancreatic ribonuclease by x-ray and neutron diffraction. *In* Biological Macromolecules and Assemblies, Vol. II. F. A. Jurnak and A. McPherson, editors. John Wiley and Co., New York. 393–439.

Wlodawer, A., L. A. Svensson, L. Sjolin, and G. L. Gilliland. 1988. Structure of phosphate-free ribonuclease A refined at 1.26 Å. *Biochemistry.* 27:2705–2717.

Wodak, S. Y., M. Y. Liu, and H. W. Wyckoff. 1977. The structure of cytidilyl (2',5') adenosine when bound to pancreatic ribonuclease S. *J. Mol. Biol.* 116:855–875.